Hindawi Publishing Corporation
ISRN Biophysics
Volume 2013, Article ID 981958, 1 page
http://dx.doi.org/10.1155/2013/981958

Retraction

Retracted: Interaction of TMPyP4, TMPyP3, and TMPyP2 with Intramolecular G-Quadruplex Formed by Promoter Region of Bcl2 and KRAS NHPPE

ISRN Biophysics

Received 15 March 2013; Accepted 15 March 2013

This article has been retracted upon the authors' request, as they have incorporated the studies of two oncogene promoter regions which form G-quadruplex complex (i.e., Bcl2 and KRAS), but the DNA considered for the studies was not from these regions. The DNA samples got mixed up, and they are from other regions of oncogene promoter. The complete ESI-MS (mass data) and the ITC (microcalorimetry data) were wrong. Since the mistake occurred at the fundamental level (i.e., at the DNA itself), the whole experiment gave wrong data. Additionally, the article was submitted for publication by the author Narayana Nagesh without the knowledge and approval of the other author Arumugam Ganesh Kumar [1].

References

[1] N. Nagesh and A. Ganesh Kumar, "Interaction of TMPyP4, TMPyP3, and TMPyP2 with intramolecular G-quadruplex formed by promoter region of Bcl2 and KRAS NHPPE," *ISRN Biophysics*, vol. 2012, Article ID 786596, 12 pages, 2012.

International Scholarly Research Network
ISRN Biophysics
Volume 2012, Article ID 786596, 12 pages
doi:10.5402/2012/786596

Research Article

Interaction of TMPyP4, TMPyP3, and TMPyP2 with Intramolecular G-Quadruplex Formed by Promoter Region of Bcl2 and KRAS NHPPE

Narayana Nagesh[1] and Arumugam Ganesh Kumar[2]

[1] *Department of Medicinal Chemistry, Centre for Cellular and Molecular Biology, Hyderabad 500007, India*
[2] *Marine Biotechnology, National Institute of Ocean Technology, Chennai 600100, India*

Correspondence should be addressed to Narayana Nagesh, nagesh5112@gmail.com

Received 5 September 2011; Accepted 2 October 2011

Academic Editors: M. P. Evstigneev and M. P. Ponomarenko

Oncogenes are rich in guanine and capable of forming quadruplex structure. Promoter regions oncogenes such as Bcl2 and KRAS NHPPE are rich in guanine content and they can form quadruplex structures. Alterations in the mode and nature of molecular binding to DNA, certainly has effect on the posttranscriptional activities. Recent experiments indicate that structure of quadruplex complex and ligand has predominant role on ligand-quadruplex DNA interaction. In order to understand the nature of each ligand interaction with quadruplex DNA, Bcl2, KRAS NHPPE quadruplex DNA interaction with three porphyrin was studied using spectroscopy, microcalorimetry and mass spectrometry. Our studies, indicate that mode of ligand interaction varies with structure, environment and concentration of ligand. Fluorescence quenching experiments show that TMPyP4 interaction is ligand concentration dependent. Job plots and ITC experiments demonstrate that four molecules of TMPyP4 and two molecules of TMPyP3, TMPyP2 interact with each quadruplex complex. Through ITC titrations, ligand binding constant are higher for TMPyP4 ($\approx 10^7\ M^{-1}$) compared to TMPyP3, TMPyP2 ($\approx 10^5\ M^{-1}$). ESI-MS experiments confirm the stoichiometry of TMPyP4 : 39Bcl2 is 4 : 1 at saturation and it is 2 : 1 in case of KRAS NHPPE quadruplex.

1. Introduction

Guanine has a unique property of aggregating with each other and form bundles in solution. It was shown earlier by Gellert et al. in the 1960s, that GMP in solution will form aggregates in presence of cations [1]. Certain regions of human genome like telomeres, promoters of oncogenes, are rich in guanine content [2–4]. Telomeres contain stretches of guanine bases and will forms bundles in presence of monovalent cations like K^+, Na^+, NH_4^+, and so forth, [5]. It has been proved that G-quadruplex structures were prevalent under *in vivo* conditions. Analyses of human genome sequence reveal that several regions in human chromosome specially the promoter region of oncogenes were rich in guanine which can form quadruplex structure. Quadruplexes are present in the promoter regions of human oncogenes [6]. Hence, any ligand which can interact with quadruplex DNA and stabilize them can act as a molecular switch and bring down cancer cells proliferation. The region a little upstream to Bcl2 P1 promoter (1386–1423 bp) was known to form quadruplex structure as it is rich in guanine content. Bcl2 protein levels were found higher in cancer cells than in normal cells. Hence Bcl2 levels were identified as a marker for cancer cell proliferation. Any ligand which can interact with quadruplex DNA and stabilize them are found to reduce the level of Bcl2 protein and bring down proliferation of cancer cells. KRAS gene is located in the chromosome 12, locus 12p12.1. The promoter of KRAS gene contains nuclease hypersensitive polypurine-polypyrimidine element (NHPPE) which is essential for transcription. NHPPE is rich in guanine content, it will form quadruplex DNA structure. Gomez et al. [7] and Thao Tran et al. [8] have performed several studies on various ligands interaction with quadruplex DNA. Recently, they have shown the antitumor activity of ligand 12459 and incorporation of 8-methylguanine in the DNA that

Table 1: Oligonucleotide sequences from Bcl2 P1 promoter and KRAS NHPPE element.

Name	1	2	3	4	5	6	7	8	9	10	11	12	13
39Bcl2	AGG	GGC	GGG	CGC	GGG	AGG	AAG	GGG	GCG	GGA	GCG	GGG	CTG
KRAS NHPPE	GGG	CGG	TGT	GGG	AAG	AGG	GAA	GAG	GGG	GAG			

improves the stability of parallel quadruplexes. For many years porphyrins were identified as suitable molecules which can interact with quadruplex DNA and stabilize them [9, 10]. But the mode and nature of each form of porphyrin interaction with quadruplex DNA are different [11]. In our earlier studies, site and mode of porphyrin molecules interaction with quadruplex DNA were shown using 2-AP fluorescence quenching [12]. Gray et al. have recently shown how fluorescence emission and quenching (by acrylamide) can be used to differentiate two closely related quadruplexes [13]. It was demonstrated that the interaction of each porphyrin varies with quadruplex DNA under different ion concentrations [14].

Quadruplex complex may exist in different forms like chair, basket, propeller, hybrid, and so forth, [15]. In the present work, it was demonstrated that parallel/antiparallel intramolecular quadruplexes formed by P1 promoter of Bcl2 and NHPPE region of KRAS interact with each porphyrin ligand in a different manner. Each porphyrin ligand interaction depends on the structure of quadruplex and the ligand, concentration, and environment of ligand.

2. Materials and Methods

2.1. Preparation of Oligonucleotide and Porphyrin Solutions. Oligonucleotides, 39Bcl2, KRAS NHPPE was obtained from BioServe India (P) Ltd., Hyderabad, India. The sequences of the four oligonucleotides used are shown in Table 1.

The two oligonucleotides were rich in guanine and they can form G-quadruplex complex. The P1 promoter region of human Bcl2 was shown to form three unique parallel/antiparallel intramolecular structures and depending upon the structure of quadruplex complex present, various binding sites will be available for interaction [16]. All the oligonucleotides stock solutions were prepared by dissolving them in 100 mM KCl BPES buffer (30 mM potassium phosphate, pH 7.0, with 100 mM KCl, pH 7.0). DNA samples were dialyzed (1000 molecular weight cutoff membrane) against two changes of buffer (1 L, 24 hours each) at 4°C. Concentration of the oligonucleotides was measured using UV-Vis spectrophotometer with molar extinction coefficients determined by using nearest neighbor calculation for single stranded DNA [17] and the absorbance of thermally denatured constructs extrapolated back to 25°C and/or a total phosphate analysis technique [18]. The extinction coefficients determined for the G-quadruplexes by these techniques are $€_{254} = 309040\,M^{-1}\,Cm^{-1}$ (39Bcl2) and $€_{260} = 317400\,M^{-1}\,Cm^{-1}$ (KRAS NHPPE), respectively.

Cationic porphyrins TMPyP2 (5, 10, 15, 20-meso-tetra (N-methyl-2-pyridyl) porphyrin) TMPyP3 (5, 10, 15, 20-meso-tetra (N-methyl-3-pyridyl) porphyrin and TMPyP4 (5, 10, 15, 20-meso-tetra (N-methyl-4-pyridyl) porphyrin were purchased from Frontier Scientific (Logan, Utah, USA). All the porphyrin drugs were used without further purification. Porphyrin solutions were prepared by dissolving weighed amount of each drug in measured volume of final dialysate from the appropriate oligonucleotide solution preparation as the buffer. Concentration of each porphyrin drug was calculated using the molar extinction coefficient $€_{424} = 2.26 \times 10^5\,M^{-1}\,Cm^{-1}$ [19] $€_{417} = 2.50 \times 10^5\,M^{-1}\,Cm^{-1}$ [20] $€_{414} = 1.82 \times 10^5\,M^{-1}\,Cm^{-1}$ [21] for TMPyP4, TMPyP3, and TMPyP2, respectively.

2.2. CD Experiments. Circular dichroism experiments were performed using JASCO 815 CD spectropolarimeter (Jasco, Tokyo, Japan). CD spectrum was recorded from 200 to 500 nm for characterizing DNA, to study the G-quadruplex-porphyrin interaction and observe for induced CD (ICD) by porphyrins. For CD experiment, 5×10^{-6} M of G-quadruplex DNA was used. To characterize porphyrin-quadruplex interaction, CD spectra were recorded at 1 : 4 and 1 : 3 molar ratio in case of quadruplex DNA : TMPyP4 and quadruplex : TMPyP2/TMPyP3, respectively. CD titrations were performed in 100 mM KBPES buffer (pH 7.0) at 25°C. Each CD spectrum was recorded thrice and the average of three scans is considered.

2.3. Fluorescence Experiments. Fluorescence emission spectra were measured at 25°C using F-4500 spectrofluorometer (Hitachi, Japan) using 1 cm path length quartz cuvette. G-quadruplex DNA samples were taken in 2 mL of 100 mM KBPES buffer (pH 7.0). Fluorescence titration was carried out at lower TMPyP4 concentration (1000 nM) to observe the effect of concentration on ligand binding. Fluorescence spectra were recorded after each addition of quadruplex DNA to the fluorescent cuvette, keeping TMPyP4 concentration constant. G-quadruplex DNA and porphyrin drug mixture volume was kept constant throughout the fluorescence titration (2 mL). After each titration, quartz cuvettes were thoroughly washed with distilled water and dilute nitric acid (approximately 0.1 N, nitric acid) to remove traces of porphyrin adhering to the walls of quartz cuvette. TMPyP4, TMPyP3, and TMPyP2 are excited at 433 nm, 417 nm, and 424 nm, respectively, and emission spectra were collected from 600 to 800 nm. Each spectrum was recorded three times and the average was considered.

2.4. UV-Visual Spectroscopic Titrations. UV-Visual spectroscopic titrations were performed using ABI UV-Vis spectrophotometer (Foster City, USA) at 25°C using 1 cm path length quartz cuvette. Stock solutions of 10 μM ligand and 10 μM of G-quadruplex DNA were prepared in 100 mM KBPES buffer (pH 7.0). Two series of solutions were used for the experiments in one part two mL of dilute G-quadruplex

DNA (10 μM) is taken in 1 cm path length quartz cuvette and twenty-five $\times$ 50 μL injections of porphyrin solution (10 μM) were added manually. In the second part, two mL of dilute ligand solution (10 μM) was taken and twenty-five $\times$ 50 μL injections of G-quadruplex DNA solution were added. Absorption spectra were collected from 350 nm to 500 nm. The quartz cells were thoroughly cleaned with distilled water and 0.1 N nitric acid to remove traces of porphyrin that are deposited on the walls of quartz cell. The difference in the absorption maxima of the Soret band was plotted versus the ligand mole fraction to generate Job plot [22, 23]. UV-Vis absorption titrations were done by adding G-quadruplex DNA stock solution (200–350 nM) in 100 mM KBPES buffer (pH 7.0) to the quartz cuvette containing approximately 1 μM ligand solution prepared in the same buffer. Preparation of G-quadruplex DNA and ligand samples were done on the same day of performing the experiment. UV spectra were collected from 200 nm to 500 nm to monitor the position of absorption band of ligand. The titrations were carried out until the ligand Soret band remains at a fixed wavelength upon five successive additions of G-quadruplex DNA.

2.5. Isothermal Titration Calorimetry (ITC). ITC experiments were performed using Microcal VP-ITC. All the ITC experiments were done by overfilling the ITC cell with approximately 1.5 mL of G-quadruplex DNA solution. DNA concentration was maintained at 20–40 μM and ligand concentration in the titration syringe was maintained at 9 $\times$ 10^{-5} M for TMPyP4 and TMPyP3 and 3 $\times$ 10^{-3} M for TMPyP2. Higher concentration of TMPyP2 was required as the heat of dilution of TMPyP2 into the G-quadruplex solution was less at lower concentration. This indicates lower binding efficiency of TMPyP2 to G-quadruplex DNA. Each time 60 injections (5 μL) of cationic porphyrin were added to ITC cell. Drug addition to G-quadruplex DNA was performed every 180 seconds. Throughout the ITC experiment, the final dialysate from the appropriate oligonucleotide was used in order to maintain heat of porphyrin dilution constant. Each ITC experiment was performed in triplicate to avoid errors generated while performing the experiment. The integrated heat/injection data obtained in each ITC titration were fitted with algorithm developed for use with Mathematica 5.0 software. The ITC titrations raw data and the fitted binding isotherms were shown in Figure 5. Values for $\Delta G1(K1)$, $\Delta G2(K2)$, ΔH°, $\Delta H2$, $-T\Delta S1$, and $-T\Delta S2$ were extracted directly from the fits.

2.6. Electrospray Ionisation Mass Spectrometry (ESI-MS). Electrospray ionization mass spectrometry (ESI-MS) was used to study the binding stoichiometry of porphyrin binding to each quadruplex complex formed by 39Bcl2 and KRAS NHPPE element. Electrospray ionization (ESI) mass spectra were recorded using an LCQ (liquid chromatography quadrupole) ion trap mass spectrometer (Thermo Finnigan, San Jose, CA, USA), equipped with an ESI source. ESI-MS experiments were carried out in negative ion mode. The data acquisition was under the control of XCalibur software (Thermo Finnigan). The typical source conditions were spray voltage, 3.5 kV; capillary voltage, -4.0 V; heated capillary temperature, 140°C; tube lens offset voltage, 20 V; sheath gas (N_2) pressure, 35 psi; aux/sweep gas pressure, 5 psi; helium was used as damping gas. For the ion trap mass analyzer, the automatic gain control (AGC) settings were 2×10^7 counts for a full-scan mass spectrum and 2×10^7 counts for a full product ion mass spectrum with a maximum ion injection time of 200 ms. All the spectra were recorded under identical experimental conditions with an average of 25–30 scans. All the samples were infused into the ESI source at a flow rate of 5 μL/min by using instrument's syringe pump. The relative intensities of free and bound DNA in mass spectra were assumed to be proportional to the relative abundance of each species in solution.

2.7. Preparation of Drug/Quadruplex DNA Complexes. TMPyP4 interaction with 39Bcl2 and KRAS NHPPE element was considered as it was known from our earlier studies, TMPyP4 can interact well with quadruplex DNA than other two isomers (TMPyP2 and TMPyP3). Hence noncovalent interactions between TMPyP4 and 39Bcl2 and KRAS quadruplex were considered. Stock solution of TMPyP4 (1 mM) was prepared in 0.1 M NH_4OAc, pH 8.5. 40 nM of TMPyP4 solution was mixed with 10 nM 39Bcl2 and KRAS NHPPE element quadruplex to get quadruplex/ligand ratio of 1 : 4 in 100 μL total volume. Prior to ESI-MS analysis, equal volume of 0.1 M NH_4OAc was added. Methanol was added to the mixture just before injection (15%) after the complexation equilibrium in ammonium acetate was established to obtain stable electrospray signal.

3. Results

3.1. Circular Dichroism of Bcl2 G-Quadruplex DNA with Cationic Porphyrins. CD spectra obtained with 39Bcl2, KRAS NHPPE region G-quadruplexes show a positive CD band near 264 nm and negative band at 240 nm in 100 mM KBPES buffer (pH 7.0). This indicates that all of them adopt parallel G-quadruplex structure [16, 24]. Cationic porphyrins alone do not exhibit circular dichroism spectra in the absence of DNA. All the three porphyrins do not show significant drug-induced CD after interaction with quadruplex DNA. However, TMPyP4 at saturation (1 : 4 quadruplex DNA : TMPyP4) exhibited a low-intensity drug-induced negative CD band in the visible region. The occurrence and magnitude of induced CD (ICD) will indicate the extent of porphyrin interaction with the G-quadruplex DNA.

In order to understand the nature of cationic porphyrins interaction with G-quadruplex DNA and to assess the effect of DNA conformation on the nature of interaction, CD spectrum was recorded with quadruplex formed by 39Bcl2 and KRAS NHPPE element and three porphyrins at saturation levels. The CD spectra recorded with 39Bcl2, KRAS NHPPE were shown in Figures 1(a) and 1(b), respectively. At saturation (1 : 4 quadruplex DNA : TMPyP4), a less intense negative induced CD band at 436 nm was noticed on increasing the TMPyP4 concentration (CD band

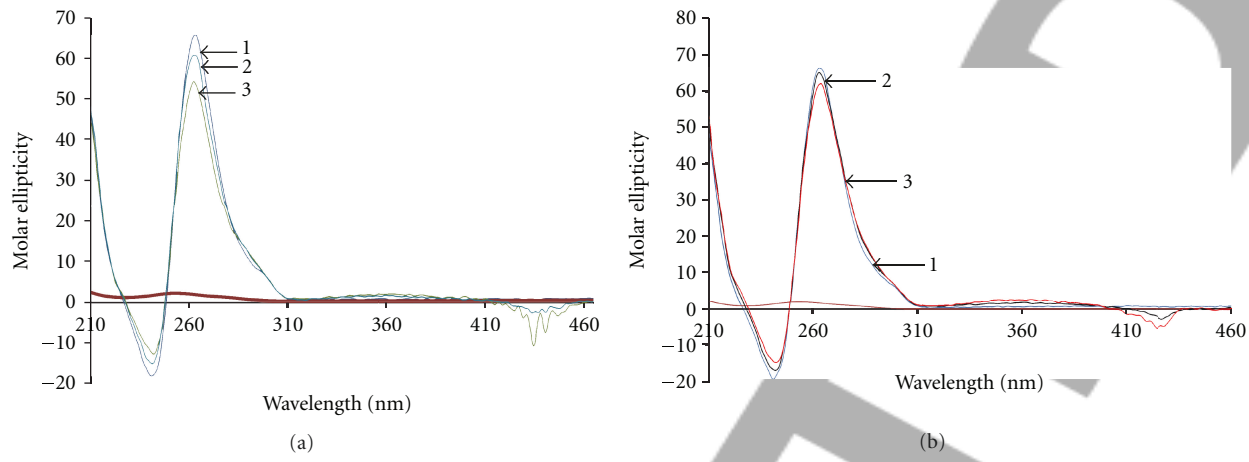

Figure 1: (a) CD spectra obtained with TMPyP4 are interacting with 39Bcl2 quadruplex DNA. Clear ICD can be seen at 463 nm on addition of 1 : 4 ratios of 39Bcl2 quadruplex DNA : TMPyP4. CD peaks labeled 1, 2, 3 corresponds to TMPyP2, TMPyP3, and TMPyP4, respectively. (b) CD spectra obtained with TMPyP4 are interacting with KRAS quadruplex DNA. Clear ICD can be seen at 463 nm on addition of 1 : 4 ratios of KRAS quadruplex DNA : TMPyP4. CD peaks labeled 1, 2, 3 corresponds to TMPyP2, TMPyP3, and TMPyP4, respectively.

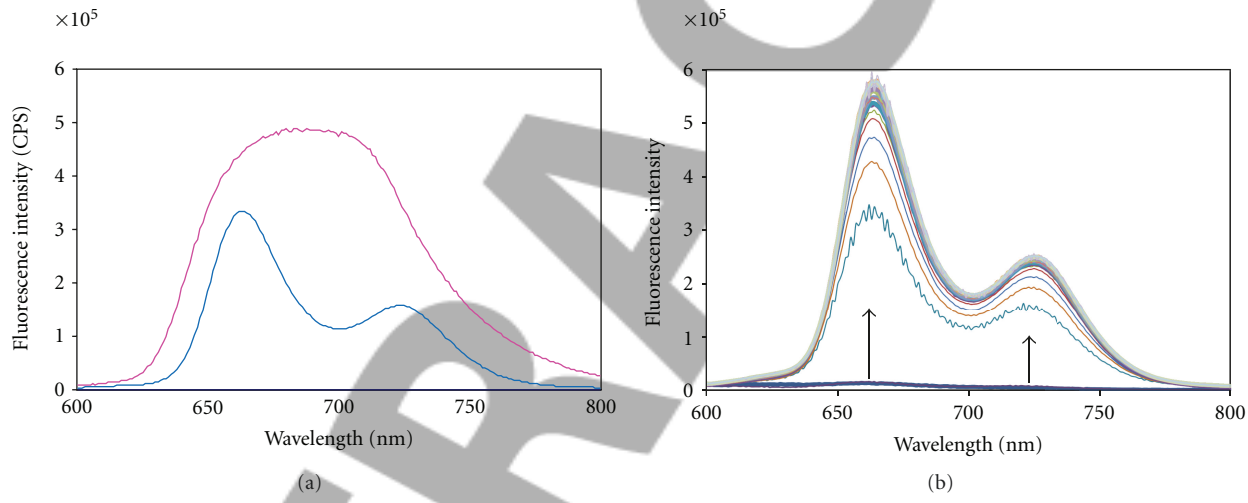

Figure 2: (a) Fluorescence emission spectra obtained for TMPyP4. Spectra 1 is before and spectra 2 after the interaction of TMPyP4 (10 μM) with Bcl2 G-quadruplex DNA. (b) Fluorescence spectra obtained with 39Bcl2 quadruplex DNA are added in gradual increments to 10 nM TMPyP4 solution.

marked 3 in Figure 1(a)). Presence of negative induced CD band at 436 nm and decrease of CD band intensity at 264 nm on addition of TMPyP4 indicate that TMPyP4 was interacting with 39Bcl2 G-quadruplex structure and it brings about small changes in the DNA conformation. Further, the position of CD bands does not shift on interaction with TMPyP3 and TMPyP2, confirming that quadruplex DNA remains in parallel conformation even after interaction with three porphyrins. On interaction with TMPyP3, a low intense ICD at 463 nm (CD band marked 2 in Figure 1(a)) was observed, whereas TMPyP2 interaction did not show induced CD at 463 nm even at saturation level (CD band marked 1 in Figure 1(a)), indicating low level of interaction with 39Bcl2 quadruplex DNA.

CD studies using quadruplex formed by KRAS NHPPE element showed variation in its interaction with three ligands. The interaction of TMPyP3 and TMPyP4 (CD bands labeled 2, 3 in Figure 1(b)) showed comparatively low-intensity ICD at 463 nm. Like with 39Bcl2 quadruplex, KRAS also did not show reduction in the intensity of 264 nm band. The intensity of CD band at 264 nm remains almost the same on addition of all three porphyrins, indicating lesser changes in the quadruplex structure on ligand interaction.

3.2. Fluorescence Spectroscopy. Fluorescence was a very sensitive technique for studying the mode of ligand interaction with quadruplex DNA. Figure 2(a) displays the emission spectra of TMPyP4 before and after the addition of Bcl2 G-quadruplex DNA. Porphyrin is complexed with DNA in solutions, which have quadruplex DNA/TMPyP4 ratios of 1 : 2+ and 1 : 4+. Results obtained on interaction of three cationic porphyrins with Bcl2 and KRAS quadruplex

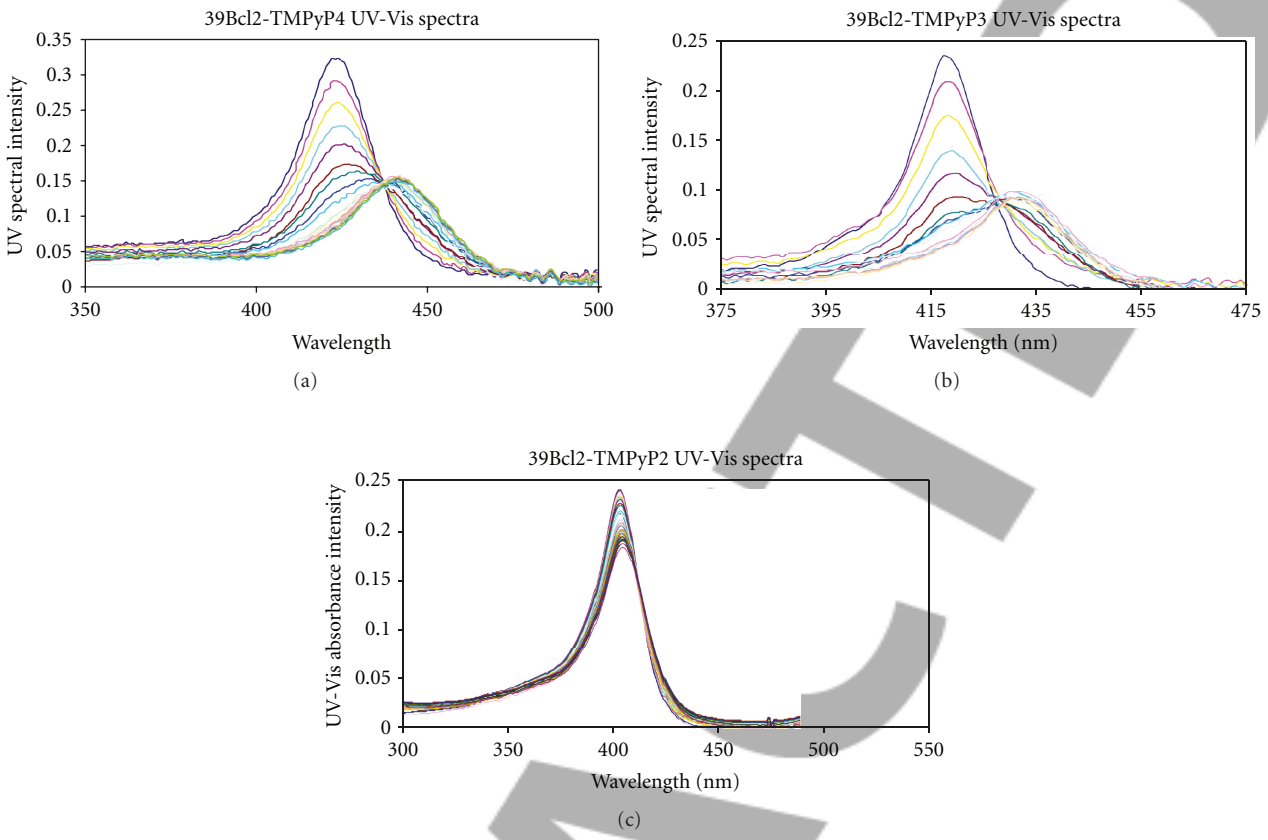

Figure 3: UV-Vis spectra of 39Bcl2 G-quadruplex DNA in 100 mM KBPES buffer (pH 7.0) on interaction with TMPyP4, TMPyP3, and TMPyP2 respectively.

DNA were shown in Table 4. From Figure 2(a) it is evident that TMPyP4 emission spectrum was getting quenched on addition of excess of porphyrin (in the concentration range of μM). But when porphyrin ligands were interacting with quadruplex DNA at lower concentration (10–1000 nM), fluorescence intensity decreases initially and on further addition of TMPyP4, fluorescence intensity gradually increases as shown in Figure 2(b). TMPyP4 emission spectrum was composed of a single very broad peak at higher ligand concentration and it splits into two peaks centered at about 665 nm and 727 nm on addition of quadruplex DNA (Figure 2(a)). Spectra for the other porphyrins (P3 and P2) exhibit two (660 and 705 nm), and three peaks (640, 660 and 705 nm) respectively (data not shown). These results, in particular the significant enhancement/quenching of the emission spectra at lower/higher porphyrin concentrations indicate that TMPyP4, when placed in the local environment of the DNA, exhibits concentration-dependent interaction. TMPyP2, TMPyP3 exhibits only reduction in the intensity of fluorescent band on addition of quadruplex DNA at low/high ligand concentration.

TMPyP4 Soret band showed slight red shift on interaction with quadruplex DNA, whereas TMPyP3, TMPyP2 does not show red shift, indicating TMPyP4 interacts better with quadruplex DNA. These conclusions are made on the considerations that binding of porphyrins to GC sites in random sequence DNA and G-quadruplex was similar. Mukundan et al. [25] has observed moderate red shift of the fluorescence emission band and hypochromicity of the emission band on interaction of tetracationic tentacle porphyrins with calf thymus DNA. Results obtained from fluorescence experiments are matching with UV-spectroscopic and ITC experimental results. The results obtained from the fluorescence titration were given in Table 4.

3.3. Binding Modes of Cationic Porphyrins by UV-Vis Spectroscopic Studies. Usually, UV-Vis absorbance is used to study the extent of ligand binding to DNA. Earlier much work has been done using UV-Vis spectroscopy to understand the nature of interaction of different ligands, drugs, and other macromolecules with DNA [12, 26–30]. Figure 3 demonstrates the changes in the absorption spectra of TMPyP2, TMPyP3, and TMPyP4 on interaction with 39Bcl2 G-quadruplex DNA. Since the profile of UV-Vis spectra obtained with 39Bcl2 and KRAS was almost similar, hence spectra recorded with KRAS quadruplex were not shown, but results were tabulated in Table 2.

Figure 3(a), shows that the Soret band has shifted from 423 nm to 441 nm (18 nm shift) in case of TMPyP4 and the isobestic point was noticed at around 436 nm. In case of TMPyP3, the Soret band has shifted from 417 nm to 431 nm (13-14 nm shift) and isobestic point was observed at around 426 nm (Figure 3(b)), whereas in the case of TMPyP2 the

Table 2: UV-Vis Absorption titration parameters for TMPyP4, TMPyP3, and TMPyP2 with four different Bcl2 and KRAS NHPPE-G-quadruplex DNA.

S. no.	Name of G-quadrupelx DNA and cationic porphyrin	Soret band shift (nm)	Isobestic point (nm)	Percentage hypochromicity
1	39Bcl2-TMPyP4	423–441	436.5	68.4%
2	39Bcl2-TMPyP3	417–431	427.0	55.0%
3	39Bcl2-TMPyP2	No shift	422.0	32.5%
4	KRAS NHPPE-TMPyP4	423–441	435.5	59.7%
5	KRAS NHPPE-TMPyP3	417–431	426.5	41.5%
6	KRAS NHPPE-TMPyP2	No shift	422.0	23.0%

Soret band hypochromicity is calculated using the fomula: % Hypochromicity = $[(€_{free} - €_{bound})/€_{free}] \times 100$. $€_{free}$ and $€_{bound}$ are the extinction coefficient of free and bound porphyrin, respectively.

Soret band does not show shift from 414 nm and an isobestic point was observed at around 422 nm (Figure 3(c)). It is clear from Figure 3(a) that in case of 39Bcl2 G-quadruplex DNA, at the end of UV-Vis titration there is a slight deviation from the isobestic point, when it is interacting with TMPyP4, indicating binding of TMPyP4 to 39Bcl2 G-quadruplex DNA involves multiple steps. Percentage of hypochromicity for each G-quadruplex DNA is calculated by following the procedure described by Wei et al. [31]. Percentage of hypochromicity of the porphyrin Soret band after interaction with both quadruplexes were in the following order TMPyP4 > TMPyP3 > TMPyP2.

3.4. Binding Stoichiometric Ratios of Cationic Porphyrins to G-Quadruplex DNA: Job Plots. The method of continuous variation analysis (Job plot) was used to determine the number of molecules of porphyrin binding to G-quadruplex DNA. Figures 4(a), 4(b), and 4(c) demonstrate Job plots obtained on TMPyP4, TMPyP3, and TMPyP2 interaction with 39Bcl2 and KRAS quadruplex DNA, respectively. Difference in the absorption maxima of the Soret band was used to generate Job plots. On careful analysis of data obtained from Job plots, it was clear that 4 molecules of TMPyP4 bind to each molecule of G-quadruplex DNA, whereas about 2 molecules of TMPyP2 or TMPyP3 bind to 1 molecule of G-quadruplex DNA. These results are consistent with ITC experimental data.

3.5. Isothermal Titration Calorimetry (ITC). ITC is a sensitive and direct microcalorimetric technique for determining the information about binding affinity, stoichiometry, and thermodynamic parameters [32]. Interaction between 39Bcl2 and KRAS G-quadruplex DNA and TMPyP4, TMPyP3 and TMPyP2 analyzed at 25°C using 100 mM KBPES (pH 7.0) buffer was documented in Figures 5(a) and 5(b). The corresponding binding isotherms shown in Figure 5, were generated by integrating the heats produced per injection with respect to time and calculated in per mole basis (as shown in Table 5). After making corrections for dilutions, the data was fitted using Origin 7.1 software to calculate thermodynamic parameters like binding constant (K), interaction enthalpy (ΔH), stoichiometry, ΔG and $-T\Delta S$. The thermodynamic parameters like, $K2$, $\Delta H2$, $\Delta G2$ and $-T\Delta S2$ were not available with TMPyP2 and TMPyP3 due to low interaction with G-quadruplex DNA.

3.6. ESI-MS Spectroscopic Studies. Quadruplex complex was always stabilized by central monovalent cations such as K^+, Na^+, or NH_4^+. The mass spectrum exhibits a typical pattern depending upon the number of cations imbedded in the quadruplex structure. It has been shown by Rosu et al. [24] that the noncovalent interactions that take place during quadruplex DNA and ligand interactions can be preserved during electrospray process, provided suitable experimental conditions are used. Hence ESI-MS spectra can be considered for studying the stoichiometry and relative binding affinities of different ligands to quadruplex DNA.

The formation of stable complex between TMPyP4 and Bcl2/KRAS NHPPE element quadruplex was clearly demonstrated by the presence of distinct peaks in the mass spectra corresponding to 1 : 1, 1 : 2, 1 : 3 and 1 : 4 39Bcl2 quadruplex DNA : TMPyP4 complex (as shown in Figure S1 in Supplementary Material available online at doi:10.5402/2012/786596), whereas in case of quadruplex formed by KRAS NHPPE, relative abundance of 1 : 1 and 1 : 2 quadruplex : TMPyP4 molecular species was seen clearly (Figure S2) in the total ligand: quadruplex DNA population. Figure 6 shows the relative abundance of each species in the solution and its composition. TMPyP4 exhibited higher affinity towards 39Bcl2 than KRAS NHPPE quadruplex, matching with ITC results. Higher interaction of TMPyP4 with 39Bcl2 may be due to variation in quadruplex folding pattern.

4. Discussion

39Bcl2 oligonucleotide contains 6 continuous stretches of guanines with one stretch of five guanines, two stretches of four guanines, and three stretches of three guanines each. KRASNHPPE element has 4 continuous stretches of guanines [33]. It was reported that 39Bcl2 could form a mixture of three distinct intramolecular G-quadruplex structures in presence of K^+ ions [34]. Hurley et al. and others [35–37] have shown that cationic porphyrins can bind to G-quadruplex DNA/duplex DNA and stabilize the structure through electrostatic interactions between positively charged nitrogen atoms of the pyridyl rings and negatively charged phosphate oxygen atoms of DNA.

On careful literature survey, certain features characterize intercalations of porphyrins to DNA. If porphyrin was intercalating to G-quadruplex DNA then it should result

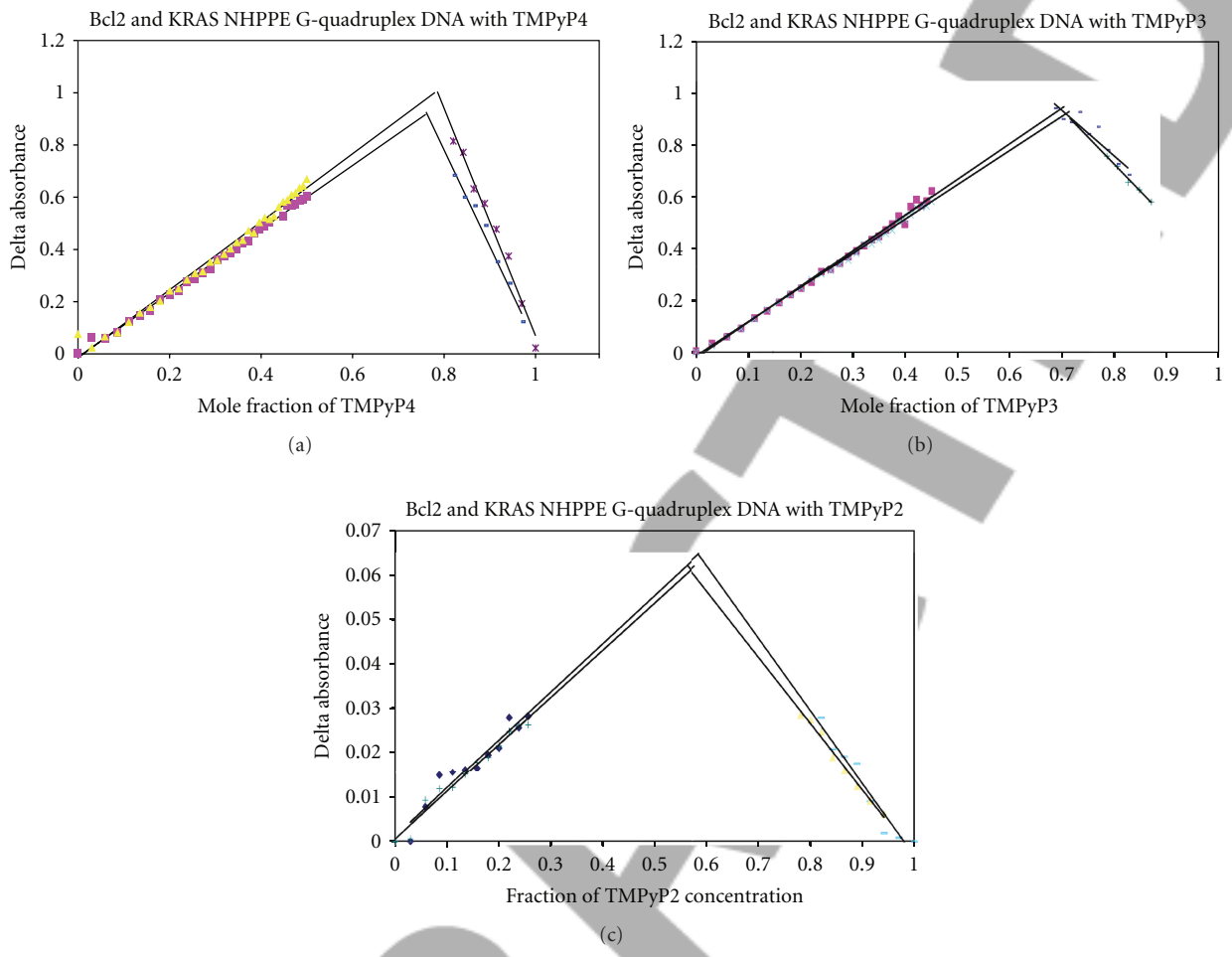

Figure 4: Job plots obtained with 39Bcl2 and KRAS G-quadruplex DNA in 100 mM KBPES buffer (pH 7.0) on interaction with TMPyP4, TMPyP3, and TMPyP2, respectively.

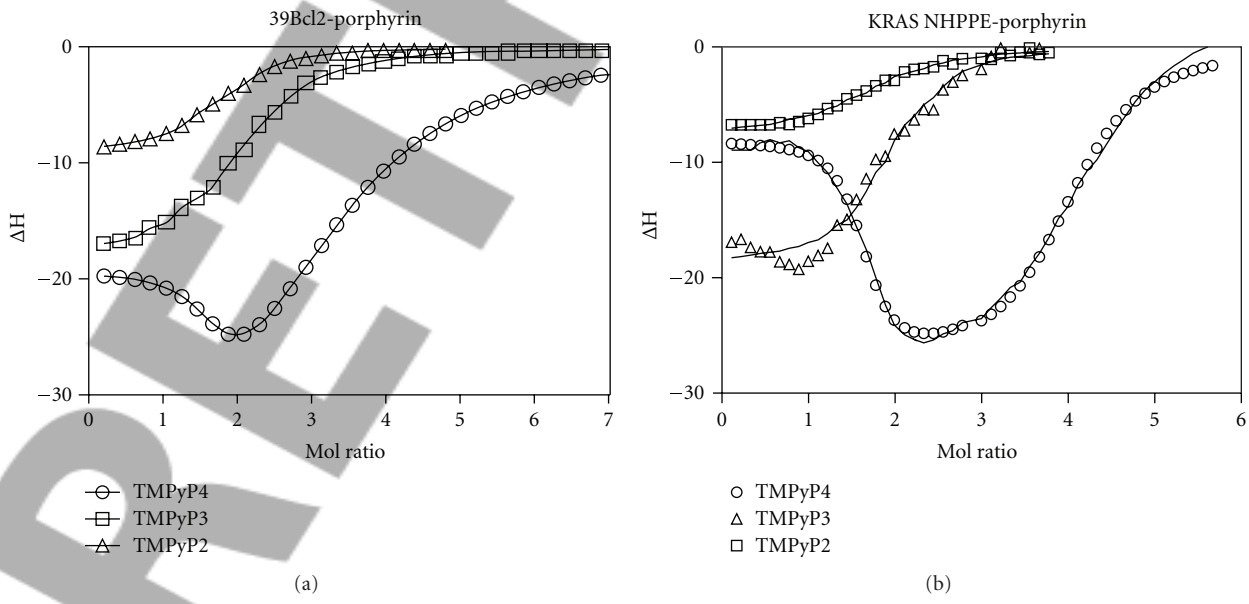

Figure 5: ITC data for titration of two G-quadruplex DNA with porphyrin solution (9×10^{-5} M of TMPyP4, TMPyP3 and 3×10^{-3} M of TMPyP2). (a) 39Bcl 2 quadruplex-porphyrin titration; (b) K RAS quadruplex-porphyrin titration.

Table 3: Data obtained from Job plot of Bcl2 and KRAS NHPPE G-quadruplex DNA with TMPyP4, TMPyP3, and TMPyP2 porphyrin drug.

S. no.	Name of G-quadrupelx DNA and porphyrin	Value of mole fraction of porphyrin matching with point of intersection	Stoichiometry between G-quadruplex DNA and porphyrin
1	39Bcl2-TMPyP4	0.80	1 : 4.00
2	39Bcl2-TMPyP3	0.68	1 : 2.10
3	39Bcl2-TMPyP2	0.62	1 : 1.63
4	KRAS NHPPE-TMPyP4	0.78	1 : 3.54
5	KRAS NHPPE-TMPyP3	0.68	1 : 2.10
6	KRAS NHPPE-TMPyP2	0.58	1 : 1.38

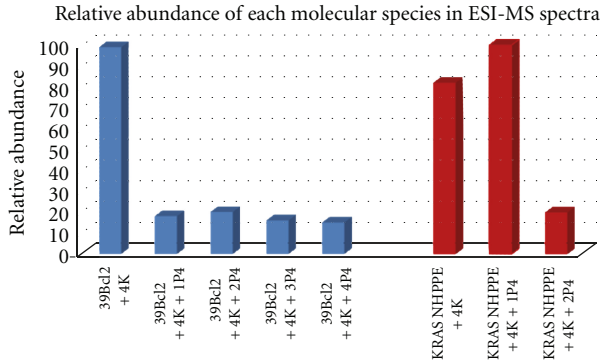

Figure 6: Bar graph indicating the population of each molecular species present in ESI-MS spectra recorded with 39Bcl2 (blue) and KRAS NHPPE (red) on TMPyP4 interaction. *X*-axis represents the relative abundance of each species and *Y*-axis represents composition of each molecular species.

in 15–18 nm red shift of the Soret band, about ≥35% hypochromicity of the porphyrin Soret band and exhibiting negative induced CD band near the porphyrin Soret region. Similarly, if the porphyrin drug was binding externally, it should result in 8–13 nm red shift of the Soret band and ≤10% of hypo- or hyperchromicity of the porphyrin Soret band. In the present study, about 18 nm and 13 nm Soret band red shift was observed when TMPyP4 and TMPyP3 were interacting with G-quadruplex DNA, whereas there was no shift of the porphyrin Soret band with TMPyP2. The average percentage of hypochromicity for TMPyP4, TMPyP3, and TMPyP2 with two different G-quadruplex DNA was approximately around 64%, 49%, and 28%, respectively (shown in Table 2). It was generally agreed that larger hypochromicities of the Soret band was an indication of better intercalation of porphyrin to DNA [38]. The hypochromicity of the Soret band in UV-Vis spectra was an indication of extent of ligand interaction with quadruplex DNA. The observations like red shift of porphyrin Soret band, hypochromicity, and presence of ICD at 436 nm indicate that TMPyP4 can interact well with both the G-quadruplex DNA. TMPyP3 has moderate interaction, whereas TMPyP2 has lowest affinity towards G-quadruplex DNA. When porphyrin was added to 39Bcl2 G-quadruplex DNA, negative cotton effect was observed at 264 nm positive CD band (Figure 1(a)), due to the rearrangement of sugar molecules in the G-quadruplex DNA. Reduction of negative cotton effect among porphyrins was in the order TMPyP4 > TMPyP3 > TMPyP2. Negative cotton effect of 264 nm CD band was not much prevalent in case of KRAS quadruplex on interaction of porphyrins, it indicates that porphyrins show better interaction with 39Bcl2 quadruplex than KRAS. On intercalation of TMPyP4 to G-quadruplex DNA, it brings smaller conformational changes in the DNA structure, without affecting its stability. Changes in percentage of hypochromicity were considered as a good measure of ligands interaction with DNA. Pasternack et al. [38] have shown that with calf thymus DNA, poly(dG-dC), and poly(dA-dT), percentage of hypochromicity and red shift of the Soret band of porphyrins increases as the G-C content of the nucleic acid increases. It was noticed that the percentage of hypochromicity when TMPyP4 interacting with quadruplex DNA, was in the order of 39Bcl2 > KRASNHPPE because the number of guanine in the DNA sequence is decreasing in the same order. Higher percentage of hypochromicity and red shift of the Soret band was observed than that reported by Haq et al. [26]. The difference in percentage of hypochromicity could be due to the variation in ionic strength of the buffer used. Decrease in percentage of hypochromicity has been reported for TMPyP4 and CuTMPyP4 on binding to calf thymus DNA with the increase in ionic strength [39].

The method of continuous variation analysis (Job plots) reveals that stoichiometry of TMPyP4 binding to 39Bcl2 was 4 : 1. At low TMPyP4 concentration, stoichiometry between porphyrin : quadruplex was 2 : 1 (data not shown) demonstrating that two porphyrin molecules first bind to the two end loops of the quadruplex structure and on addition of excess porphyrin, two more molecules will intercalate between the stacks of G-tetrad. Results from fluorescence spectroscopic and ITC experiments support the data obtained with UV-Vis experiments. Freyer et al. [30] reported similar observation while studying TMPyP4 interaction with c-MYC NHE III promoter. In case of TMPyP3 the stoichiometry between porphyrin and G-quadruplex DNA is 2 : 1. From ITC it was evident that TMPyP3 has a low level of affinity compared to TMPyP4. Though the binding efficiency was low for TMPyP2, two molecules may bind to G-quadruplex DNA. Results obtained from the Job plots of two quadruplexes on interaction with TMPyP2, TMPyP3, and TMPyP4 were shown in Table 3.

Our recent studies with mutant 2-aminopurine substituted G-quadruplex DNA structures, having larger end

Table 4: Fluorescence spectroscopic data obtained for TMPyP4, TMPyP3, and TMPyP2 with Bcl2 and KRAS NHPPE-G-quadruplex DNA.

S. no.	Name of G-quadrupelx DNA and porphyrin	% Fluorescence hypochromicity	Concentration of G-quadruplex DNA
1	39Bcl2-TMPyP4	28.78%	306 nM
2	39Bcl2-TMPyP3	53.07%	306 nM
3	39Bcl2-TMPyP2	12.56%	306 nM
4	KRAS NHPPE-TMPyP4	17.05%	218 nM
5	KRAS NHPPE-TMPyP3	21.05%	218 nM
6	KRAS NHPPE-TMPyP2	14.18%	218 nM

% Fluorescence hypochromicity (% FH) $= [(F_p - F_{bp})/F_p] \times 100$, where F_p is the fluorescence intensity of free porphyrin and F_{bp} is the fluorescence intensity of bound porphyrin.

loop, reveal that TMPyP4 first binds to the end loop and later intercalates between the two G-tetrad stacks present in the central portion of G-quadruplex DNA structure. At higher TMPyP4/quadruplex ratios (at porphyrin concentrations higher than 10^{-4} to 10^{-3} M), fluorescence emission intensities reduce on addition of ligand (Figure 2(a)). But at low TMPyP4 : quadruplex DNA ratio (1000 nM), initially the fluorescence intensity decreases, but on further addition of quadruplex DNA, emission intensity begins to increase (Figure 2(b)). We speculate that, at low porphyrin concentration, TMPyP4 is in monomer form, initially it binds to the end loop and on further increase of ligand concentration, it will intercalate between two quartets [40]. The initial decrease in fluorescence intensity was due to binding of TMPyP4 to the end loop of quadruplex complex. Increase of fluorescence emission intensities, on further addition of quadruplex DNA may be due to π-π energy transfer between the ligand and two stacks of quadruplex DNA. At higher TMPyP4 concentration, due to ligand aggregation, it binds externally to quadruplex complex. On binding externally, ligand fluorescence will be quenched by the surrounding solvent molecules. It was observed in both the quadruplexes. Chen et al. [41] have recently demonstrated that, at higher concentration and in presence of crowding agents like PEG200/glycerol, TMPyP4 exhibits lesser ability to stabilize quadruplex complex.

Not only the concentration of ligand, but also changes in the hydrophobic environment around the drug molecules affected the fluorescence emission intensities. Mukundan et al. [25] made similar observation when porphyrin interacts with calf thymus DNA. Hudson et al. reports that intercalation of copper cationic porphyrin to DNA prevents quenching of fluorescence emission peak by the solvent [42]. When TMPyP3 was interacting with both quadruplex complexes, there is a continuous fall in the fluorescence, indicating that it is binding exterior. With TMPyP2, differences in fluorescence intensities are very small. The slight variation in delta fluorescence values among the two G-quadruplex DNA complex studied was due to the difference in their structure formed by each oligonucleotide.

The change in fluorescence intensity of porphyrin drug, in the absence of DNA and at saturating levels, provides the percentage of fluorescence hypochromicity. From Table 4 it is clear that fluorescence hypochromicity among the three porphyrin drugs decreases in the order TMPyP3 > TMPyP4 > TMPyP2. Table 4 shows maximum fluorescence hypochromicity for TMPyP3. Fluorescence quenching of TMPyP3 was maximum because most of the TMPyP3 ligands prefer to bind externally to quadruplex DNA and get quenched by surrounding water molecules. Fluorescence hypochromicity data demonstrates that a small fraction of TMPyP2 molecules will be binding externally and getting quenched by the surrounding water molecules. There are two reasons for lowest fluorescence hypochromicity by TMPyP2, (i) it has low binding affinity to G-quadruplex DNA and (ii) the bound TMPyP2 molecules are being quenched by water, as it is binding externally to G-quadruplex DNA. TMPyP4 exhibits moderate fluorescence hypochromicity, because, the reduction in fluorescence intensity by solvent quenching was compensated by enhancement of fluorescence intensity through π-π electronic interactions between ligand and bases in quadruplex DNA on intercalation. Here, fluorescence band hypochromicity was calculated based on the method proposed by Schneider et al. [43].

Wei et al. [31] has recently reported the change in the G-quadruplex DNA conformation on intercalation of TMPyP4 using spectroscopic methods. Scheidt et al. [44] has shown that 4-N-methyl pyridyl groups at the para positions of TMPyP4 are nearly perpendicular to the plane of porphyrin core. For interaction of TMPyP4 with G-quadruplex DNA, it is necessary for the 4-N-methyl pyridyl groups in para position to rotate and attain coplanar position. Hence, for intercalation between the G-tetrads, TMPyP4 requires to move two tetrads stacks little away from each other [45]. Movement of two stacks apart from each other brings about slight change in the conformation of G-quadruplex DNA. Due to these reasons, the intensity of CD bands 264 nm changes after TMPyP4 interaction with 39Bcl2 quadruplex DNA. On addition of TMPyP3 to G-quadruplex DNA, there is a little change in the negative induced CD indicating TMPyP3 exhibits no or lesser degree of intercalation with G-quadruplex DNA. The bulky N^+-CH_3 groups in TMPyP3 were placed in meta position and its freedom of rotation is restricted to some extent. Hence TMPyP3 prefers end loop binding than intercalation. From CD and fluorescence experiments, it is evident that TMPyP3 prefers external binding to G-quadruplex DNA, whereas TMPyP2 shows neither induced CD nor brings change to the intensity of positive or negative CD bands (negative cotton effect) indicating the low level of interaction with G-quadruplex DNA. In case of TMPyP2, the N^+-CH_3 groups are in ortho position. Hence,

Table 5: ITC data of Bcl2 P1 promoter and KRAS NHPPE quadruplexes interaction with TMPyP2, TMPyP3, and TMPyP4 ligands.

ITC-derived thermodynamic parameters	39Bcl2 quadruplex DNA			KRAS NHPPE quadruplex DNA		
	TMPyP4	TMPyP3	TMPyP2	TMPyP4	TMPyP3	TMPyP2
$K_1 \times 10^{-8}$	0.360	0.256	0.0699	0.324	0.253	0.0578
ΔG_1 (kcal/mol)	−9.16	−6.87	−5.97	−8.32	−6.35	−5.73
ΔH_1 (kcal/mol)	−4.24	−3.97	−0.60	−3.82	−3.46	−0.57
$-T\Delta S_1$ (kcal/mol)	−4.52	−3.47	−6.09	−8.27	−3.21	−5.97
$K_2 \times 10^{-6}$	0.91	—	—	0.87	—	—
ΔG_2 (kcal/mol)	−6.52	—	—	−6.12	—	—
ΔH_2 (kcal/mol)	−8.97	—	—	−11.52	—	—
$-T\Delta S_2$ (kcal/mol)	−2.94	—	—	−1.79	—	—

Table 6: ESI-MS experimental details indicating the presence of different populations of 39Bcl2 and KRAS quadruplex species after interaction with TMPyP4 at saturation molar ratio.

S. no.	Interacting quadruplex	Interacting ligand	Ratio of quadruplex : ligand	Composition and charge of the complex	Designated mass of the peak	Relative abundance of each peak
(1)	39Bcl2	TMPyP4	1 : 0	$[Q + 4K]^{10-}$	1259	99
(2)	39Bcl2	TMPyP4	1 : 1	$[Q + 4K + 1P4]^{10-}$	1396	18
(3)	39Bcl2	TMPyP4	1 : 2	$[Q + 4K + 2P4]^{10-}$	1533	20
(4)	39Bcl2	TMPyP4	1 : 3	$[Q + 4K + 3P4]^{10-}$	1668	15
(5)	39Bcl2	TMPyP4	1 : 4	$[Q + 4K + 4P4]^{10-}$	1805	14
(6)	KRAS	TMPyP4	1 : 0	$[Q + 4K - 10H]^{-16}$	599	82
(7)	KRAS	TMPyP4	1 : 1	$[Q + 4K + 1P4]^{-12}$	928	95
(9)	KRAS	TMPyP4	1 : 2	$[Q + 4K + 2P4]^{-11}$	1136	20

it cannot rotate and exhibit intercalation with G-quadruplex DNA.

ITC titrations were done with two quadruplexes and the results obtained were shown in Table 5. From the results, it was clear that TMPyP4 interaction with quadruplex occurs in two ways. One is a very fast interaction process (mode 1), which takes place in combination of contribution from enthalpy (−1.7 to −4.2 kcal/mol) and significant and favorable entropy (−4.0 to −8.0 kcal/mol). The second process (mode 2), which was a relatively slower process, proceeds with more significant enthalpy (−7.0 to −12.0 kcal/mol) contribution and a smaller entropy range (−2 to +3.5 kcal/mol). Analyzing the ITC results, the energy profiles shows that interaction of TMPyP3 and TMPyP2 takes place with one binding mode closer to higher affinity binding (mode 1) of TMPyP4, considering the relative entropy and enthalpy contribution to the overall binding free energy change.

It may be due to the binding of porphyrin drugs to the surface of DNA (external binding) or end staking to quadruplex DNA. Results with ITC indicate the order of priority for mode 1 binding was in TMPyP4 > TMPyP3 ≫ TMPyP2. It occurs due to the binding of nonplanar ligands (like TMPyP3 and TMPyP2) externally, which cannot interact with quadruplex DNA by staking between the two orderly placed tetrads. The second process is best explained as it is enthalpy driven. Binding of a planar molecule between the two orderly placed tetrads takes place with a typical exothermic enthalpy change due to increased π-π staking interaction between the interacting ligand and the DNA bases [46–50]. We speculate that the second process which is significantly enthalpy driven is more likely an "intercalation process."

Noncovalent interaction between quadruplex DNA and porphyrin and stoichiometry of ligand interacting with 39Bcl2 and KRAS NHPPE element was well demonstrated by ESI-MS studies. The nature of ligand interaction and stoichiometry of ligand interaction with each quadruplex was not similar (as shown in Figure 6), it may be due to the variation in the structure and folding pattern of each quadruplex. Initial TMPyP4 interaction with KRAS NHPPE quadruplex was higher compared to the affinity of second ligand binding to quadruplex complex.

Relative abundance of quaduplex : TMPyP4 species in each of the ESI-MS spectra (Supplementary Material S1 and S2) indicate the presence of higher population of 1 : 1 and 1 : 2 forms of 39Bcl2 (approximately 33%) compared to 1 : 3 and 1 : 4 forms (around 29% in case of 39Bcl2). Results obtained in ESI-MS experiment were shown in Table 6. From the ESI-MS and ITC results we speculate that TMPyP4 interaction with 39Bcl2 occurs in two different modes, one with higher affinity and other with lower affinity. The higher affinity interaction occurs at lower quadruplex : TMPyP4 ratios (1 : 1 and 1 : 2), whereas lower affinity interaction occurs at higher quadruplex : TMPyP4 ratios (1 : 3 and 1 : 4). The initial higher affinity binding may be end loop binding and the interaction at higher molar ratios was through intercalation.

In case of KRAS NHPPE quadruplex, the initial ligand biding ($Q + 4K + 1P4$) takes place with higher affinity (more than 90% of the population will exist in 1 : 1 ratio) maybe due to higher percentage of end loop binding at lower molar ratios. Presence of ($Q + 4K + 2P4$) species was comparatively lesser, because of variation in the folding pattern of each quadruplex. All the mass spectroscopic experiments were carried out at low concentration. At higher molar ratios KRAS quadruplex may exhibit 1 : 3 and 1 : 4 molar ratio complexes in equilibrium with other. These results indicate that ligand interaction was not similar with all the quadruplex DNA. In the present study, TMPyP4 has better interaction with quadruplex formed by 39Bcl2 compared to KRAS. It may be useful in designing and development of suitable drugs for cancer, based on ligand-quadruplex DNA interaction.

5. Conclusions

From spectroscopic, microcalorimetric, and mass experiments, it is clear that cationic porphyrins prominently exhibit two different modes of binding to G-quadruplex DNA. One is the higher affinity external/end groove binding and the second lower affinity, intercalation. The mode of binding depends on the structure and concentration of ligand and conformation of quadruplex. ITC and fluorescence results indicate that TMPyP4 exhibit end groove binding at low porphyrin concentration (in the monomeric form) and external binding accompanied by intercalative binding at higher drug concentration. TMPyP3 and TMPyP2 bind to end loops of G-quadruplex DNA. Job plots and ITC titration results demonstrate that at saturation levels, four molecules of TMPyP4 and two molecules of TMPyP2 and TMPyP3 interact with Bcl-2/KRASNHPPE G-quadruplex DNA. Percentage of fluorescence hypochromicity falls in the order 39Bcl2 > KRASNHPPE, indicating the linear relationship between the length of quadruplex forming oligonucleotides, with hypochromicity. ESI-MS experimental results show that TMPyP4 interaction with quadruplex DNA depends on the folding pattern of DNA and interaction is concentration dependent.

Acknowledgment

N. Nagesh is thankful to Dr. Ch Mohan Rao, Director, CCMB, Hyderabad, India, for his encouragement and for allowing to use the facilities in the institute.

References

[1] M. Gellert, M. N. Lipsett, and D. R. Davies, "Helix formation by guanylic acid," *Proceedings of the National Academy of Sciences of the United States of America*, vol. 48, pp. 2013–2018, 1962.

[2] J. E. Johnson, J. S. Smith, M. L. Kozak, and F. B. Johnson, "In vivo veritas: using yeast to probe the biological functions of G-quadruplexes," *Biochimie*, vol. 90, no. 8, pp. 1250–1263, 2008.

[3] J. L. Huppert, "Hunting G-quadruplexes," *Biochimie*, vol. 90, no. 8, pp. 1140–1148, 2008.

[4] N. Maizels, "Dynamic roles for G4 DNA in the biology of eukaryotic cells," *Nature Structural and Molecular Biology*, vol. 13, no. 12, pp. 1055–1059, 2006.

[5] S. Burge, G. N. Parkinson, P. Hazel, A. K. Todd, and S. Neidle, "Quadruplex DNA: sequence, topology and structure," *Nucleic Acids Research*, vol. 34, no. 19, pp. 5402–5415, 2006.

[6] J. Popiołkiewicz, K. Polkowski, J. S. Skierski, and A. P. Mazurek, "In vitro toxicity evaluation in the development of new anticancer drugs—Genistein glycosides," *Cancer Letters*, vol. 229, no. 1, pp. 67–75, 2005.

[7] D. Gomez, N. Aouali, A. Londoño-Vallejo et al., "Resistance to the short term antiproliferative activity of the G-quadruplex ligand 12459 is associated with telomerase overexpression and telomere capping alteration," *Journal of Biological Chemistry*, vol. 278, no. 50, pp. 50554–50562, 2003.

[8] P. L. Thao Tran, A. Virgilio, V. Esposito, G. Citarella, J. L. Mergny, and A. Galeone, "Effects of 8-methylguanine on structure, stability and kinetics of formation of tetramolecular quadruplexes," *Biochimie*, vol. 93, no. 3, pp. 399–408, 2010.

[9] J. Seenisamy, S. Bashyam, V. Gokhale et al., "Design and synthesis of an expanded porphyrin that has selectivity for the c-MYC G-quadruplex structure," *Journal of the American Chemical Society*, vol. 127, no. 9, pp. 2944–2959, 2005.

[10] I. M. Dixon, F. Lopez, J. P. Estève et al., "Porphyrin derivatives for telomere binding and telomerase inhibition," *ChemBioChem*, vol. 6, no. 1, pp. 123–132, 2005.

[11] M. J. Carvlin and R. J. Fiel, "Intercalative and nonintercalative binding of large cationic porphyrin ligands to calf thymus DNA," *Nucleic Acids Research*, vol. 11, no. 17, pp. 6121–6139, 1983.

[12] N. Nagesh, R. Buscaglia, J. M. Dettler, and E. A. Lewis, "Studies on the site and mode of TMPyP4 interactions with Bcl-2 promoter sequence G-quadruplexes," *Biophysical Journal*, vol. 98, no. 11, pp. 2628–2633, 2010.

[13] R. D. Gray, L. Petraccone, R. Buscaglia, and J. B. Chaires, "2-aminopurine as a probe for quadruplex loop structures," *Methods in Molecular Biology*, vol. 608, pp. 121–136, 2010.

[14] N. Nagesh, V. K. Sharma, A. Ganesh Kumar, and E. A. Lewis, "Effect of ionic strength on porphyrin drugs interaction with quadruplex DNA formed by the promoter region of C-myc and Bcl2 oncogenes," *Journal of Nucleic Acids*, vol. 2010, Article ID 146418, 9 pages, 2010.

[15] Y. He, R. D. Neumann, and I. G. Panyutin, "Intramolecular quadruplex conformation of human telomeric DNA assessed with ^{125}I-radioprobing," *Nucleic Acids Research*, vol. 32, no. 18, pp. 5359–5367, 2004.

[16] J. Dai, T. S. Dexheimer, D. Chen et al., "An intramolecular G-quadruplex structure with mixed parallel/antiparallel G-strands formed in the human BCL-2 promoter region in solution," *Journal of the American Chemical Society*, vol. 128, no. 4, pp. 1096–1098, 2006.

[17] G. D. Fassman, "Nucleic acids," in *Handbook of Biochemistry and Molecular Biology*, CRC Press, Cleveland, Ohio, USA, 1975.

[18] G.E. Plum, *Determination of Oligonucleotide Molar Extinction Coefficients in Current Protocols in Nucleic Acid Chemistry*, vol. 7.3, John Wiley & Sons, New York, NY, USA, 2000.

[19] R. F. Pasternack, P. R. Huber, P. Boyd et al., "On the aggregation of meso-substituted water-soluble porphyrins," *Journal of the American Chemical Society*, vol. 94, no. 13, pp. 4511–4517, 1972.

[20] K. Kalyanasundaram, "Photochemistry of water-soluble porphyrins: comparative study of isomeric tetrapyridyl- and tetrakis(N-methylpyridiniumyl)porphyrins," *Inorganic Chemistry*, vol. 23, no. 16, pp. 2453–2459, 1984.

[21] P. Hambright, T. Gore, and M. Burton, "Synthesis and characterization of new isomeric water-soluble porphyrins. Tetra(2-N-methylpyridyl)porphine and tetra(3-N-methylpyridyl)porphine," *Inorganic Chemistry*, vol. 15, no. 9, pp. 2314–2315, 1976.

[22] L. R. Keating and V. A. Szalai, "Parallel-stranded guanine quadruplex interactions with a copper cationic porphyrin," *Biochemistry*, vol. 43, no. 50, pp. 15891–15900, 2004.

[23] W. Likussar and D. F. Boltz, "Theory of continuous variations plots and a new method for spectrophotometric determination of extraction and formation constants," *Analytical Chemistry*, vol. 43, no. 10, pp. 1265–1272, 1971.

[24] F. Rosu, E. De Pauw, and V. Gabelica, "Electrospray mass spectrometry to study drug-nucleic acids interactions," *Biochimie*, vol. 90, no. 7, pp. 1074–1087, 2008.

[25] N. E. Mukundan, G. Pethö, D. W. Dixon, M. S. Kim, and L. G. Marzilli, "Interactions of an electron-rich tetracationic tentacle porphyrin with calf thymus DNA," *Inorganic Chemistry*, vol. 33, no. 21, pp. 4676–4687, 1994.

[26] I. Haq, J. O. Trent, B. Z. Chowdhry, and T. C. Jenkins, "Intercalative G-tetraplex stabilization of telomeric DNA by a cationic porphyrin," *Journal of the American Chemical Society*, vol. 121, no. 9, pp. 1768–1779, 1999.

[27] N. V. Anantha, M. Azam, and R. D. Sheardy, "Porphyrin binding to quadruplexed T_4G_4," *Biochemistry*, vol. 37, no. 9, pp. 2709–2714, 1998.

[28] R. F. Pasternack, E. J. Gibbs, and J. J. Villafranca, "Interactions of porphyrins with nucleic acids," *Biochemistry*, vol. 22, no. 23, pp. 5409–5417, 1983.

[29] M. A. Sari, J. P. Battioni, D. Dupré, D. Mansuy, and J. B. Le Pecq, "Interaction of cationic porphyrins with DNA: importance of the number and position of the charges and minimum structural requirements for intercalation," *Biochemistry*, vol. 29, no. 17, pp. 4205–4215, 1990.

[30] M. W. Freyer, R. Buscaglia, K. Kaplan, D. Cashman, L. H. Hurley, and E. A. Lewis, "Biophysical studies of the c-MYC NHE III1 promoter: model quadruplex interactions with a cationic porphyrin," *Biophysical Journal*, vol. 92, no. 6, pp. 2007–2015, 2007.

[31] C. Wei, G. Jia, J. Yuan, Z. Feng, and C. Li, "A spectroscopic study on the interactions of porphyrin with G-quadruplex DNAs," *Biochemistry*, vol. 45, no. 21, pp. 6681–6691, 2006.

[32] J. E. Ladbury and B. Z. Chowdhry, "Sensing the heat: the application of isothermal titration calorimetry to thermodynamic studies of biomolecular interactions," *Chemistry and Biology*, vol. 3, no. 10, pp. 791–801, 1996.

[33] S. Cogoi, M. Paramasivam, V. Filichev, I. Géci, E. B. Pedersen, and L. E. Xodo, "Identification of a new G-quadruplex motif in the *KRAS* promoter and design of pyrene-modified G4-decoys with antiproliferative activity in pancreatic cancer cells," *Journal of Medicinal Chemistry*, vol. 52, no. 2, pp. 564–568, 2009.

[34] T. S. Dexheimer, D. Sun, and L. H. Hurley, "Deconvoluting the structural and drug-recognition complexity of the G-quadruplex-forming region upstream of the bcl-2 P1 promoter," *Journal of the American Chemical Society*, vol. 128, no. 16, pp. 5404–5415, 2006.

[35] E. M. Rezler, J. Seenisamy, S. Bashyam et al., "Telomestatin and diseleno sapphyrin bind selectively to two different forms of the human telomeric G-quadruplex structure," *Journal of the American Chemical Society*, vol. 127, no. 26, pp. 9439–9447, 2005.

[36] H. Han, D. R. Langley, A. Rangan, and L. H. Hurley, "Selective interactions of cationic porphyrins with G-quadruplex structures," *Journal of the American Chemical Society*, vol. 123, no. 37, pp. 8902–8913, 2001.

[37] P. Weisman-Shomer, E. Cohen, I. Hershco et al., "The cationic porphyrin TMPyP4 destabilizes the tetraplex form of the fragile X syndrome expanded sequence d(CGG)n," *Nucleic Acids Research*, vol. 31, no. 14, pp. 3963–3970, 2003.

[38] R. F. Pasternack, E. J. Gibbs, and J. J. Villafranca, "Interactions of porphyrins with nucleic acids," *Biochemistry*, vol. 22, no. 10, pp. 2406–2414, 1983.

[39] G. Dougherty, J. Pilbrow, A. Skorobogaty, and R. Kreilick, "EPR and ENDOR study of selected porphyrin- and phthalocyanine-copper complexes," *Journal of Physical Chemistry*, vol. 96, no. 23, pp. 9132–9139, 1992.

[40] K. Kano, H. Minamizono, T. Kitae, and S. Negi, "Self-aggregation of cationic porphyrins in water. Can π-π stacking interaction overcome electrostatic repulsive force?" *Journal of Physical Chemistry A*, vol. 101, no. 34, pp. 6118–6124, 1997.

[41] Z. Chen, K. W. Zheng, Y. H. Hao, and Z. Tan, "Reduced or diminished stabilization of the telomere G-quadruplex and inhibition of telomerase by small chemical ligands under molecular crowding condition," *Journal of the American Chemical Society*, vol. 131, no. 30, pp. 10430–10438, 2009.

[42] B. P. Hudson, J. Sou, D. J. Berger, and D. R. McMillin, "Luminescence studies of the intercalation of Cu(TMpyP4) into DNA," *Journal of the American Chemical Society*, vol. 114, no. 23, pp. 8997–9002, 1992.

[43] J. H. Schneider, J. Odo, and K. Nakamoto, "Interactions of water-soluble metalloporphyrins with nucleic acids studied by resonance Raman spectroscopy," *Nucleic Acids Research*, vol. 16, no. 21, pp. 10323–10338, 1988.

[44] W. R. Scheidt, "Stereochemistry of low-spin cobalt porphyrins. III. The crystal structure and molecular stereochemistry of bis(piperidine)-$\alpha,\beta,\gamma,\delta$-tetraphenylporphinatocobalt(II)," *Journal of the American Chemical Society*, vol. 96, no. 1, pp. 84–89, 1974.

[45] L. A. Lipscomb, F. X. Zhou, S. R. Presnell et al., "Structure of a DNA-porphyrin complex," *Biochemistry*, vol. 35, no. 9, pp. 2818–2823, 1996.

[46] J. B. Chaires, "Analysis and interpretation of ligand—DNA binding isotherms," *Methods in Enzymology*, vol. 340, pp. 3–22, 2001.

[47] D. Suh and J. B. Chaires, "Criteria for the mode of binding of DNA binding agents," *Bioorganic and Medicinal Chemistry*, vol. 3, no. 6, pp. 723–728, 1995.

[48] J. Ren and J. B. Chaires, "Sequence and structural selectivity of nucleic acid binding ligands," *Biochemistry*, vol. 38, no. 49, pp. 16067–16075, 1999.

[49] K. M. Hyun, S. D. Choi, S. Lee, and S. K. Kim, "Can energy transfer be an indicator for DNA intercalation?" *Biochimica et Biophysica Acta*, vol. 1334, no. 2-3, pp. 312–316, 1997.

[50] J. B. Chaires, "A thermodynamic signature for drug-DNA binding mode," *Archives of Biochemistry and Biophysics*, vol. 453, no. 1, pp. 26–31, 2006.